ELSEVIER

Journal of Pharmaceutical and Biomedical Analysis
30 (2002) 151–159

JOURNAL OF
PHARMACEUTICAL
AND BIOMEDICAL
ANALYSIS

www.elsevier.com/locate/jpba

^{1}H-NMR study of the effect of acetonitrile on the interaction of ibuprofen with human serum albumin

Zhusheng Ji [a], Hanzhen Yuan [b], Maili Liu [b], Jiming Hu [a,*]

[a] *Department of Analysis-Measurement Science, Wuhan University, Wuhan 430072, People's Republic of China*
[b] *Laboratory of Magnetic Resonance and Atomic and Molecular Physics, Wuhan Institute of Physics and Mathematics, The Chinese Academy of Sciences, Wuhan 430071, People's Republic of China*

Received 19 March 2002; received in revised form 15 April 2002; accepted 18 April 2002

Abstract

The effect of acetonitrile (ACN) on the low-affinity interaction between human serum albumin (HSA) and ibuprofen (IBP) was studied using ^{1}H-NMR techniques. Both chemical shift and relaxation measurements showed the addition of ACN to the solutions decreased the binding affinity of IBP to HSA and reduced the hydrophobic interaction between them. The self-diffusion coefficients of IBP were measured as a function of the drug concentration at different ACN concentrations. The association constant, K_a, for ligand–HSA complexes and the number of binding sites, n, are evaluated by the application of Langmuir isotherm. The results indicated that the value of n was about 38 without ACN, and about 26 with ACN concentration 12% (v/v%). The decreased binding capacity of IBP to HSA in the presence of ACN was mainly attributed to the competition of ACN with IBP to the low-affinity binding sites of HSA molecule.

Keywords: Ibuprofen; Human serum albumin; Acetonitrile; NMR; Relaxation; Diffusion

1. Introduction

Human serum albumin (HSA) is the most abundant protein in blood. The diversity of chemical functions present at the surface of the protein allows it to interact with a broad range of substances like drugs. Extensive studies on different aspects of drug–HSA interactions are still in progress because the binding process can affect drug transport to tissues and hence the compound's therapeutic effect, toxicity and pharmacokinetics [1]. It is generally believed that there are two main kinds of ligand binding to a HSA molecule [2]. One of these is high-affinity binding with one or two specific binding sites and with the association constant in the order of 10^{4}–10^{6} M^{-1} [3]. Numerous investigations have been carried out on the high-affinity interaction [4]. The other is low-affinity binding with tens of binding sites [5,6]. It has been found that many compounds, such as pyrimidine bases, are involved in the low-affinity binding interaction, especially when the ligand concentration is much higher than that of HSA in

* Corresponding author. Tel.: +86-27-8788-2136; fax: +86-27-8788-2661
E-mail address: jmhu@whu.edu.cn (J. Hu).

0731-7085/02/$ - see front matter
PII: S0731-7085(02)00225-X

the solution [7]. In this case the high-affinity binding sites are fully saturated and the interactions between the ligand in excess and HSA are governed by the low-affinity and high-capacity binding [8].

Due to these interactions, high-performance liquid chromatography (HPLC) using immobilized HSA on a suitable support as a stationary phase has been developed for separating structurally very closely related compounds, particularly for chiral separations [9]. Along with its analytical application, HSA based liquid chromatographic phase has also been used to study binding interactions between small molecules and protein [10]. Capillary electrophoresis (CE) using HSA additive to the background electrolyte (BGE) as selector has also successfully been applied for both separations and studies of protein-drug interactions [10,11]. Owing to the highly complex structure of HSA molecule, it is extremely difficult to obtain any detailed insight into the mechanisms of binding and retention by the HSA stationary phase. More recently, Zhivkova et al. [12] studied the drug–HSA interaction using HPLC method with diazepam and diclofenac as model compounds. They concluded that the retentions due to binding at low-affinity sites are 97 and 76% for diazepam and diclofenac, respectively. It proves that the low-affinity interaction between ligands and HSA play an important role in the retention of small molecules at HSA stationary phase.

Both in HPLC and CE using HSA as selector, it is common to use significant proportions of organic modifiers, such as methanol, ethanol, 1-propanol, 2-propanol or acetonitrile (ACN), to improve the peak shape and reduce the retention of many compounds to acceptable values. Recently, some investigators have studied the influence of organic modifiers on the ligands–HSA interaction using HPLC or CE method [13–15]. But the information is still limited for the understanding of the usefulness of organic modifiers.

NMR has been extensively used as a useful method for obtaining information on the interactions between macromolecules and small ligand molecules [16]. However, in studies on the high-affinity binding between HSA and drug molecules, the application of this spectroscopic method has been limited to small proteins [17]. When the drug molecules are tightly bound to the high-affinity binding sites of a large protein as HSA, the line-broadening effect makes the drug NMR signal non-observable [8]. However, NMR is suitable for studies of the weak low-affinity interaction, where the drug molecules in free and bound states are in fast exchange on the NMR time scale. In such a case, NMR parameters of drug molecules, such as chemical shifts, relaxation rates and self-diffusion coefficients are the weighted-average of the free and bound states. In this paper, we use NMR technique to study the influence of ACN, which is widely used as an organic modifier, on the low-affinity interaction between drug and HSA. A non-steroidal anti-inflammatory drug, ibuprofen (IBP), is used as a model compound because of its relatively well-characterized binding properties with this protein. Some investigations show that IBP is a site II selective binding ligand to HSA with association constant in the order of 10^5 M^{-1} [18,19]. Therefore, IBP has been used intensively as a probe in studying the high-affinity binding properties of enantiomers to HSA. Recent studies with NMR indicated that HSA also has low-affinity binding sites for IBP [20–23].

2. Experimental

2.1. Materials and sample preparations

HSA (essentially fatty-acid free fraction V) and IBP sodium salt were all purchased from Sigma Chemical Co. (Poole, Dorset, UK) and without further purification. All other chemicals used were of analytical grade. Seven samples containing ACN at concentrations of 0, 1, 3, 6, 9, 12 and 15% (v/v) were prepared. The ACN concentration used in the work was limited to 15% (v/v%) to prevent the denaturation of HSA [24]. The concentrations of HSA and IBP were respectively kept at 0.5 and 50 mM for these samples. Such high concentration ratio ensures the high-affinity binding sites being saturated. Another two sets of samples were prepared at the concentrations of ACN 0 and 12%, respectively, containing 10, 20,

30, 40, 50, 60 and 75 mM of IBP and 0.5 mM of HSA, which corresponded to the HSA-to-IBP molar concentration ratios of 1:20, 1:40, 1:60, 1:80, 1:100, 1:120 and 1:150. The pH values of all samples were kept at 7.4 with 0.2 M phosphate buffer. The solvent contained 10% D_2O for the NMR spectrometer field–frequency lock.

2.2. Apparatus

All ^{1}H-NMR experiments were performed on a Bruker ARX-500 spectrometer at 25 °C (298 K), using a probe tuned at 500.13 MHz. The NMR spectrometer is equipped with a pulsed field gradient accessory capable of delivering z-field gradients up to 490 mT m^{-1}.

2.3. NMR relaxation and diffusion coefficient measurements

Spin lattice relaxation times were measured using the standard inversion–recovery method [25]. The diffusion coefficients were determined by a bipolar gradient longitudinal eddy-current delay (LED) method [26]. The water signal was effectively suppressed using phase-shift presaturation during both the pre-pulse delay and the recovery period [20]. For all diffusion coefficient measurement, a diffusion time (T_D) of 500 ms, an eddy current recovery time (T_E) of 40 ms and a relaxation delay (T_R) of 2 s were used. A series of spectra were measured on each of the solutions with gradient strength in the range of 8–60% of the maximum output of gradient amplitude on steps of 4% with sine-shaped gradients of 1 ms duration at the base of the pulse width. Typically, 64 or 96 transients were acquired into 16 K data points over a spectral width of 6000 Hz. The time domain data was multiplied by a cosine function to improve the signal-to-noise ratio and zero-filled by a factor of two prior to Fourier transformation. The spectral baseline was carefully corrected to remove the effect of the overlapped protein resonance. The areas of NMR peaks were used to derive the diffusion coefficients with the equation

$$A(b) = A(0)\exp(-bD) \quad (1)$$

where $b = (2\alpha\gamma\delta G)^2(\Delta - \delta/3)$, γ is the ^{1}H gyromagnetic ratio, δ and G are the duration and strength of the gradient pulse, Δ is the effective diffusion time, $\alpha = 2/\pi$ is a gradient shape factor for the sine-shaped gradient, $A(b)$ and $A(0)$ are the NMR signal areas in the presence and absence of the gradient pulses and D is the diffusion coefficient [27].

3. Results and discussion

3.1. The influence of ACN on the Binding of IBP to HSA

Fig. 1 shows ^{1}H-NMR spectra of IBP in pure solution (Fig. 1a) and solutions with an IBP-to-HSA ratio of 100:1 at the absence of ACN (Fig. 1b) and at the ACN concentration 6 (Fig. 1c), and 15% (Fig. 1d). Due to the relatively low-concentration and broad lineshape, the resonances from HSA were close to the baseline. No obvious chemical shifts and lineshape changes can be observed in the solutions containing only IBP at the corresponding ACN concentration range (data not shown). When HSA was added, the signals from IBP experienced line broadening and all the chemical shifts drift up-field (Fig. 1b). These changes were caused by the molecular interaction between IBP and HSA. Principally, the chemical shift is a parameter determined by local magnetic field, which is associated with the circulation electrons that surround the nucleus. This field generally opposes the external applied field. The up-field drift of chemical shift meant the effective field at the proton of IBP was decreased after IBP bound to HSA. This implied that the protons in the bound and free IBP had different chemical shifts. However, there was no extra IBP peak observed in the IBP–HSA solutions with and without ACN. This reveals the existence of fast chemical exchange between the bound and free forms of IBP on the chemical shift time scale. As the concentration of ACN increase, all the chemical shifts drift back toward the direction of absence of HSA (Fig. 1c and d). This meant that the interaction between IBP and HSA was decreased as the addition of ACN to the solution.

The systematic chemical shift changes ($\Delta\delta$) of side-chain methyl protons (H-3, H-10) and aromatic protons (H-5, H-6) of IBP in IBP–HSA solution as a function of the ACN concentration were plotted in Fig. 2, where the chemical shift of these protons with the absence of ACN was taken as reference. As it is shown in Fig. 1, the chemical shift changes increased for all these signals in IBP molecule as the ACN concentration increased. It can be seen that there is linear correlation between ACN concentration added and chemical shift changes, which clearly show a position-dependence. The slopes of the best-fit lines were 3.58 ± 0.14, 3.92 ± 0.13, 3.26 ± 0.11 and 4.29 ± 0.11 for H-5, H-6, H-3 and H-10, respectively, with all the correlation coefficients > 0.995. These meant that the H-10, which located at isobutyl group in IBP molecule, was the most seriously affected as ACN was added.

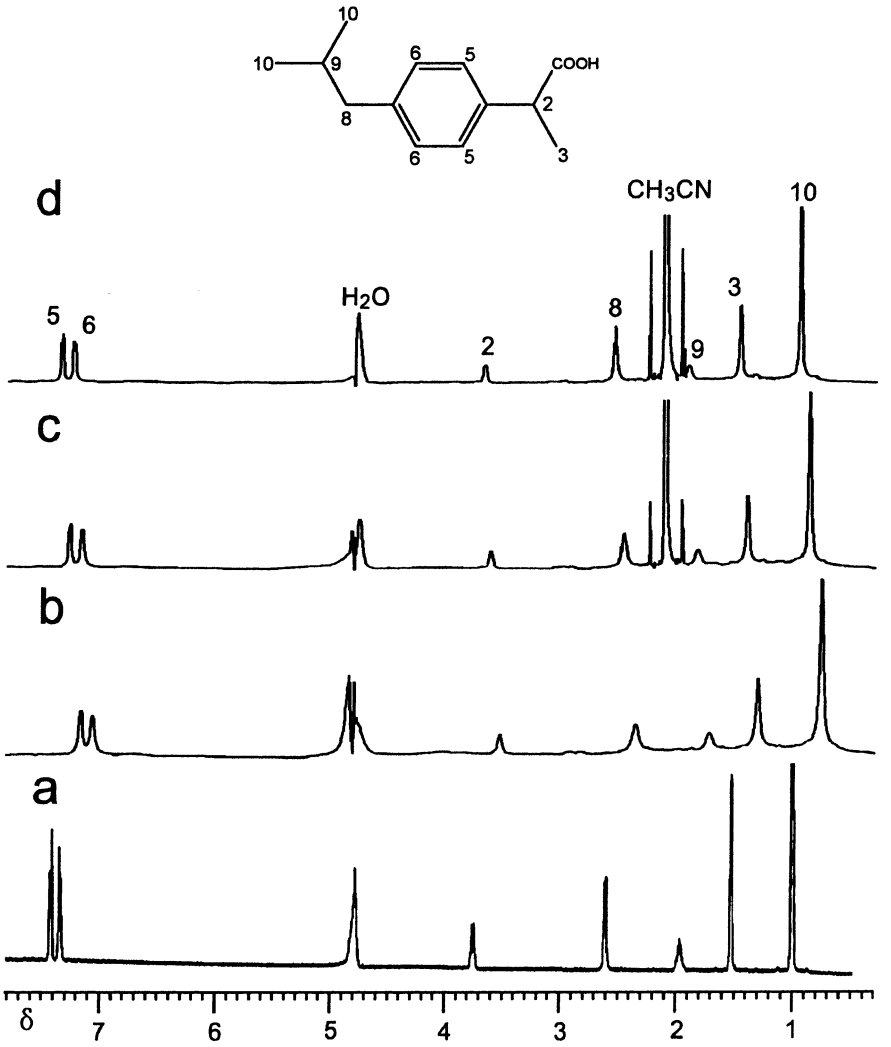

Fig. 1. ^{1}H-NMR spectra of IBP: (a) pure solution (50 mM). (b) Solution containing 50 mM IBP and 0.5 mM HSA with IBP–HSA ratio of 100:1. (c) Same as b but at the ACN concentration 6% (v/v%). (d) Same as b but at the ACN concentration 15% (v/v%) with resonance assignments. Chemical shifts are referenced to HDO (4.800 ppm).

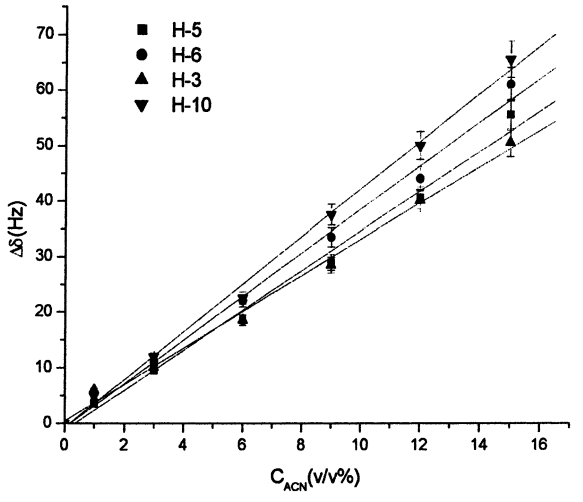

Fig. 2. The chemical shift changes ($\Delta\delta$) of H-3, H-10, H-5 and H-6 of IBP in IBP–HSA solution with the ACN concentration (C_{ACN}). The straight lines show linear correlation between ACN concentration and chemical shift changes.

Fig. 3a shows the changes of longitudinal relaxation rates (ΔR_1) of H-3, H-10, H-5 and H-6 of IBP in IBP-HSA solution with various ACN concentration, where the longitudinal relaxation rates with the absence of ACN was taken as reference.

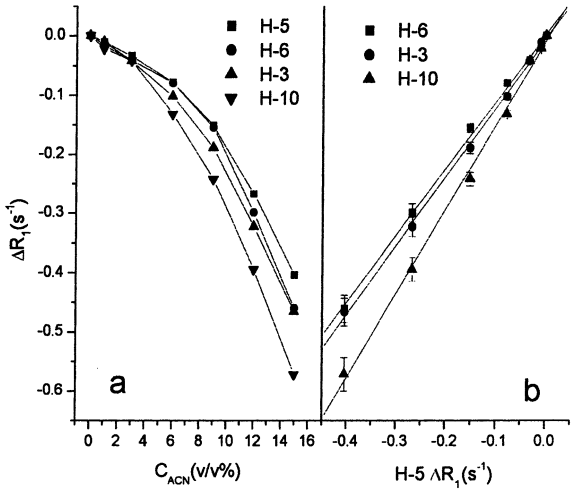

Fig. 3. (a) The changes of longitudinal relaxation rates (ΔR_1) of H-3, H-10, H-5 and H-6 of IBP in IBP–HSA solution as a function of the ACN concentration. (b) Correlation between the changes of longitudinal relaxation rates of H-3, H-10, H-6 and that of H-5.

Similar to the chemical shifts, the R_1 decreased for all these protons as the concentration of ACN increased. The decreased relaxation rates provided another evidence of the decreased interaction between IBP and HSA. The relaxation can be related to the rotational correlation time and hence the relative mobility of the small molecule. The decrease of the relaxation rates meant the motion of the IBP molecule got fast and the IBP–HSA interaction was weakened. The changes of longitudinal relaxation rates also show a position-dependence. The R_1 of H-10 decreased faster as the ACN concentration increased than that of other protons. For comparison of the variation of R_1 values, the ΔR_1 of H-3, H-6 and H-10 versus that of H-5 were shown in Fig. 3b, where straight lines were obtained with slopes of 1.13 ± 0.02, 1.16 ± 0.02 and 1.42 ± 0.03 for H-6, H-3 and H-10, respectively, and with all the correlation coefficients > 0.998. These also showed that the H-10 was the most seriously affected by the increase of ACN concentration.

From the chemical shift and relaxation rates analysis, one may draw two conclusions. First, the addition of organic modifiers into the solution obviously decreases the low-affinity interaction between drug and HSA. This may be one of the most important reasons for the reduction of the solute retention. Second, the isobutyl protons of the IBP molecule are the most seriously affected by the increase of organic modifier concentration. It is apparent from the structure of IBP molecule that isobutyl group is more hydrophobic than propanoic group where a carboxyl anion exists. The isobutyl protons was effected the most seriously meant the addition of ACN to the solution mainly reduce the hydrophobic interaction between ligands and HSA. It is generally held that the effect of organic modifier on the separation of compounds by HSA stationary phase is due to a decrease in the nonpolar interactions between ligands and HSA [28]. Ahmed et al. [14] have investigated the effect of organic modifiers on the retention and enantiomeric separations of benzoin and propiomazine by CE method with HSA as a chiral selector. They explained the primary function of the organic modifiers is to compete with the compounds in binding to the non-polar

residues of HSA and, therefore, reduce the hydrophobic interaction between them. Our experimental results verified this explanation.

3.2. Determination of binding sites and the apparent association constant

Langmuir isotherm is an equation used to describe the dynamical equilibrium between adsorption and desorption of gaseous molecules at solid surfaces. It is known that this equation can be applied not only to gas–solid interaction but also to liquid–solid interaction. Jacobson et al. have used the equation to determine the equilibrium isotherms between ligands and BSA stationary phase [29]. In the paper, Langmuir adsorption isotherm was applied to evaluate the dynamic parameters of the ligand–HSA complex for the purpose to quantitatively describe the effect of organic modifiers on the low-affinity interaction between ligand and HSA. The binding process can be described by the equation

$$\text{Drug} + \text{HSA} \underset{k_{-1}}{\overset{k_1}{\rightleftarrows}} \text{Complex} \tag{2}$$

Suppose that each HSA molecule has a maximum of n sites available for accepting ligand molecules, and the total concentration of HSA and ligand in solution are C_P and C_L, respectively. We have the following relations:

$$nC_P = [L_B] + [P] \tag{3}$$

$$C_L = [L_F] + [L_B] \tag{4}$$

where [P] is the concentration of free binding sites of HSA, $[L_F]$, $[L_B]$ are the concentration of free and bound ligand, respectively. From the two assumption of the Langmuir isotherm [30], the following equations can be derived:

$$\text{Rate of adsorption} = k_1[L_F](nC_P - [L_B]) \tag{5}$$

$$\text{Rate of desorption} = k_{-1}[L_B] \tag{6}$$

When the equilibrium between adsorption and desorption is established, the right side of the above two equations must equal. Then the relative analogous to Langmuir isotherm can be established:

$$\frac{[L_B]}{nC_P} = K_a \frac{[L_F]}{1 + K_a[L_F]} \tag{7}$$

or

$$[L_B] = \frac{nC_P K_a[L_F]}{1 + K_a[L_F]} \tag{8}$$

where $K_a = k_1/k_{-1} = [L_B]/[L_F](nC_P - [L_B])$, is the association constant for the equilibrium formation of drug–HSA complex.

When data for $[L_B]$ and $[L_F]$ are available, plotting $[L_B]$ versus $[L_F]$ and fitting the curve with Eq. (8) will simultaneously yield the two parameters, n and K_a.

$[L_B]$ and $[L_F]$ can be obtained by NMR measurement. The observed NMR parameters, the relaxation rates or self-diffusion coefficients, should be a weighted average of the contributions from bound and free molecules and should be expressed in the form [31]:

$$Y_{obs} = X_B Y_B + X_F Y_F = X_B(X_B - Y_F) + Y_F \tag{9}$$

where Y is relaxation rates or self-diffusion coefficients, and X_B and X_F are the fractions of the bound and free drug molecules defined by $[L_B]/C_L$ and $[L_F]/C_L$, respectively. By measuring a series of Y_{obs} data as a function of the concentration ratio C_P/C_L and by extrapolating the observed Y_{obs} data respectively to zero and infinite C_P/C_L, Y_B and Y_F, $[L_B]$ and $[L_F]$ can be determined.

Take H-3 for example. The measured self-diffusion coefficients (D_{obs}) for H-3 of IBP without ACN and with 12% ACN at various IBP concentrations are shown in Table 1. The results of these two sets of solutions show that as the ratio of C_P/C_L is increased, the observed self-diffusion coefficients D_{obs} are correspondingly decreased. Extrapolating D_{obs} to infinite C_P/C_L and to zero C_P/C_L, respectively, it can be obtained that $D_B = 0.50 \times 10^{-10}$ m^2 s^{-1} and $D_F = 5.57 \times 10^{-10}$ m^2 s^{-1} for solutions without ACN, $D_B = 3.60 \times 10^{-10}$ m^2 s^{-1} and $D_F = 8.98 \times 10^{-10}$ m^2 s^{-1} for solutions with ACN concentration 12%. Based on the fast exchange model in Eq. (9) and the definition of X_B and X_F, values of $[L_B]$ and $[L_F]$, which are also listed in Table 1, can be determined. The plots of the values of $[L_B]$ and $[L_F]$ for solutions with and without ACN are shown in Fig. 4. Fitting the data to Eq. (8), the association con-

Table 1
Measured self-diffusion coefficients (D_{obs}) for H-3 of IBP without ACN and with 12% ACN (v/v%) in 0.5 mM HSA solutions

C_P/C_L	0% ACN			12% ACN		
	D_{obs} (10^{-10} m^2 s^{-1})	$[L_B]$ (mM)	$[L_F]$ (mM)	D_{obs} (10^{-10} m^2 s^{-1})	$[L_B]$ (mM)	$[L_F]$ (mM)
0.0067	4.41	17.19	57.81	8.12	11.95	63.05
0.0083	4.14	16.98	43.02	7.95	11.50	48.50
0.010	3.90	16.45	33.55	7.79	11.10	38.90
0.013	3.59	15.61	24.39	7.53	10.81	29.19
0.017	3.19	14.11	15.89	7.23	9.75	20.25
0.025	2.68	11.41	8.59	6.75	8.29	11.71
0.050	2.01	7.02	2.98	6.13	5.29	4.71

stant K_a and the number of binding sites n are simultaneously obtained.

Table 2 shows the apparent association constant of IBP binding to HSA and number of binding sites on HSA by NMR self-diffusion coefficient measurements of H-5, H-6, H-3 and H-10 at ACN concentration 0 and 12%. The average association constants and number of binding sites are $K_a = 1.85 \times 10^2$ M^{-1}, $n = 38$ without ACN and $K_a = 1.34 \times 10^2$ M^{-1}, $n = 26$ at the ACN concentration 12%. It shows that the HSA molecule with the presence of ACN has less low-affinity binding sites for IBP than with the absence of ACN. The decreased binding sites of IBP to HSA can be explained by the fact of competing of ACN with IBP to the low-affinity binding sites of HSA molecule. The fact that organic modifiers, such as ACN, can reduce the retention of many compounds to acceptable values at HSA stationary phase may be associated to this reason. The results also show that the apparent association constant of IBP–HSA complex is smaller in the presence of ACN than in the absence of ACN. The small changes in HSA conformation and binding capacity, which is induced by the organic modifiers entrapment in the interior hydrophobic region of the protein, may contribute to this phenomenon. As stated above, this work mainly deals with the effect of organic modifiers on the weak low-affinity interaction between small molecules and HSA. Therefore, it is not surprising to have tens of low-affinity binding sites on one HSA molecule, and to have the apparent association constant of three orders of magnitude smaller than that of the high-affinity binding.

Both diffusion and relaxation measurements can be used for determining the dynamical parameters of ligand–HSA complex. However, the relaxation data may differ greatly for different functional groups in a molecule because relaxation mainly provides information for local structures and local dynamics. On the contrary, diffusion is a property characterizing the whole molecule or the whole complex and the measured data are close to each other for all signals in the same molecule. From this point of view, diffusion measurements are more suitable in the study [21].

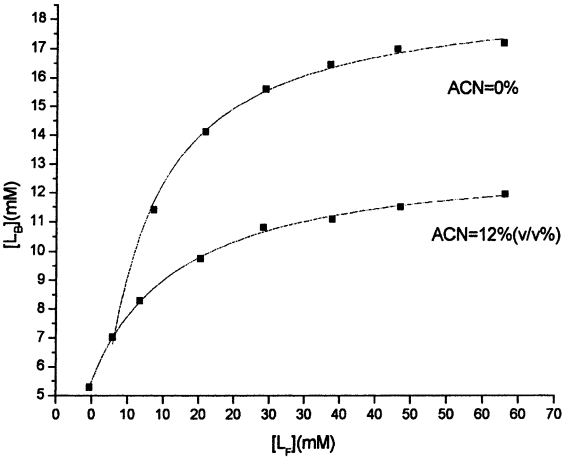

Fig. 4. Plots of $[L_B]$ vs. $[L_F]$ for solutions without ACN and at ACN concentration 12% (v/v%). Solid curve is the simulated result using Langmuir isotherm equation, Eq. (8).

Table 2
Determination of apparent association constant of IBP binding to HSA and number of binding sites on HSA by NMR diffusion (D) measurements for solutions without ACN and at ACN concentration 12% (v/v%)

Proton	0% ACN		12% ACN	
	K_a (10^2 M^{-1})	n	K_a (10^2 M^{-1})	n
H-3	1.88 ± 0.08	38	1.42 ± 0.04	26
H-10	1.74 ± 0.11	38	1.53 ± 0.09	27
H-5	1.90 ± 0.15	39	1.18 ± 0.06	26
H-6	1.88 ± 0.11	37	1.22 ± 0.07	25

4. Conclusions

In the present work, we have studied the effect of organic modifiers on the low-affinity interaction between IBP and HSA using ^{1}H-NMR method. High concentration ratios of IBP to HSA were used for the study to ensure that the molecular interaction was governed by the low-affinity and high-capacity binding. Significant changes in chemical shift and spin-lattice relaxation rates of IBP protons in the HSA solution were observed when the concentration of ACN was increased from 0 to 15%. The results suggested that the addition of ACN obviously decreased the low-affinity binding capacity of IBP to HSA and reduce the hydrophobic interaction between them. With a fast reversible and site-independent binding model, the number of binding sites of the IBP–HSA complex, calculated from the self-diffusion coefficient data, was about 38 without ACN to 26 with the ACN concentration 12% (v/v%). This suggested that the decreased binding capacity at the presence of ACN could be attribute to a decrease in the number of binding sites.

Acknowledgements

This work is supported by the grants from the National Natural Science Foundation of China (NSFC: # 29925515, # 29725307, # 29875021 and # 29875034) and the grant from State Key Laboratory of Magnetic Resonance and Atomic and Molecular Physics.

References

[1] B. Fichtl, A.V. Nieciecki, K. Walter, Adv. Drug Res. 20 (1991) 117–165.
[2] U. Kragh-Hansen, Pharmacol. Rev. 33 (1981) 17–53.
[3] M. Dockal, D.C. Carter, F. Rüker, J. Biol. Chem. 274 (1999) 29303–29310.
[4] J. Oravcová, B. Böhs, W. Lindner, J. Chromatogr. B 677 (1996) 1–28.
[5] R.B. Parker, C.L. Williams, S.C. Laizure, J.J. Lima, J. Pharmacol. Exp. Ther. 275 (1995) 605–610.
[6] R. Zini, D. Morin, P. Jouenne, J.P. Tillement, Life Sci. 43 (1988) 2103–2115.
[7] A. Sulkowska, Appl. Spectrosc. 51 (1997) 428–432.
[8] T. Oida, J. Biochem. 100 (1986) 99–113.
[9] S.G. Allenmark, J. Chromatogr. A 666 (1994) 167–179.
[10] D.S. Hage, S.A. Tweed, J. Chromatogr. B 699 (1997) 499–525.
[11] D.K. Lloyd, A.-F. Aubry, E.D. Lorenzi, J. Chromatogr. A 792 (1997) 349–369.
[12] Z. Zhivkova, V. Russeva, J. Chromatogr. B 707 (1998) 143–149.
[13] E. Peyrin, Y.C. Guillaume, C. Guinchard, Anal. Chem. 70 (1998) 4235–4240.
[14] A. Ahmed, D.K. Lloyd, J. Chromatogr. A 766 (1997) 237–244.
[15] J. Yang, D.S. Hage, J. Chromatogr. A 766 (1997) 15–25.
[16] J.S. Gounarides, A. Chen, M.J. Shapiro, J. Chromatogr. B 725 (1999) 79–90.
[17] J.M. Johnson, E.M. Meiering, J.E. Wright, J. Pardo, A. Rosowsky, G. Wagner, Biochemistry 36 (1997) 4399–4411.
[18] T. Itoh, Y. Saura, Y. Tsuda, H. Yamada, Chirality 9 (1997) 643–649.
[19] D.S. Hage, T.A.G. Noctor, I.W. Wainer, J. Chromatogr. A 693 (1995) 23–32.
[20] M.-L. Liu, J.K. Nicholson, J.C. Lindon, Anal. Commun. 34 (1997) 225–228.
[21] R.-S. Luo, M.-L. Liu, X.-A. Mao, Appl. Spectrosc. 53 (1999) 776–779.
[22] Y.-H. Ma, M.-L. Liu, X.-A. Mao, J.K. Nicholson, J.C. Lindon, Magn. Reson. Chem. 37 (1999) 269–273.
[23] C.-G. Li, M.-L. Liu, C.-H. Ye, Appl. Magn. Reson. 19 (2000) 178–186.
[24] A. Shibukawa, T. Nakagawa, M. Miyake, N. Nishimura, H. Tanaka, Chem. Pharm. Bull. 37 (1989) 1311–1315.
[25] M.L. Martin, G.J. Martin, J.-J. Delpuech, Practical NMR Spectroscopy, Heyden, London, 1980, pp. 244–275.
[26] D. Wu, A. Chen, C.S. Johnson, J. Magn. Reson. A 115 (1995) 260–264.
[27] E.O. Stejskal, J.E. Tanner, J. Chem. Phys. 42 (1965) 288–292.
[28] B. Loun, D.S. Hage, Anal. Chem. 66 (1994) 3814–3822.
[29] S. Jacobson, S. Golshan-Shirazi, G. Guiochon, J. Am.

Chem. Soc. 112 (1990) 6492–6498.
[30] P.W. Atkins, Processes at solid surfaces, in: Physical Chemistry, third ed., Oxford University Press, Oxford, 1986, pp. 762–789.
[31] A.J. Lennon, B.E. Chapman, P.W. Kuchel, Bull. Magn. Reson. 17 (1995) 224–225.